Automatic tree species recognition with quantitative structure models

Markku Åkerblom[1], Pasi Raumonen[1], Raisa Mäkipää[2], and Mikko Kaasalainen[1]

[1]Department of Mathematics, Tampere University of Technology, P.O. Box 553, 33101, Tampere, Finland
[2]Natural Resources Institute Finland (Luke), Vantaa, P.O. Box 18, FI-01301 Vantaa, Finland

February 13, 2018

Abstract

We present three robust methods to accurately and automatically recognize tree species from terrestrial laser scanner data. The recognition is based on the use of quantitative structure tree models, which are hierarchical geometric primitive models accurately approximating the branching structure, geometry, and volume of the trees. Fifteen robust tree features are presented and tested with all different combinations for tree species classification. The classification methods presented are k-nearest neighbours, multinomial regression, and support vector machine based approaches. Three mainly single-species forest plots of Silver birch, Scots pine and Norway spruce, and two mixed-species forest plots located in Finland and a total number of trees over 1,200 were used for demonstration. The results show that by using single-species forest plots for training and testing, it is possible to find a feature combination between 5 and 15 features, that results in an average classification accuracy above 93 % for all the methods. For the preliminary mixed-species forest plot testing, accuracy was lower but the classification approach presented potential to generalize to more diverse cases. Moreover, the results show that the post-processing of terrestrial laser scanning data of multi-hectare forest, from tree extraction and modelling to species classification, can be done automatically.

Keywords: tree species recognition, terrestrial laser scanning, quantitative structure model, tree reconstruction

1 Introduction

Large multi-hectare areas of forests with thousands of trees can now be measured quickly with terrestrial laser scanning (TLS) (Calders et al., 2015a). This kind of massive-scale remote sensing of trees requires that most, if not all, post-processing steps are done automatically. In addition to the geometric and volumetric data, an important piece of information that can be determined from the point clouds is the tree species. For example, the species have an effect on the greenhouse gas exchange of a tree (Meier et al., 2016), and measuring the change in biodiversity is related to the number of species and their distribution. Thus, automatic and reliable tree species recognition would be an essential step to make the massive-scale remote sensing from TLS data practical.

There are a number of published studies that use TLS data for tree species recognition: Haala et al. (2004) used the combination of TLS and high-resolution panoramic images to make a comparison of the bark textures of four trees. Their results show that the texture is a candidate for classification as it seems to stay similar in a stem, but differs between stems. However, the approach was not tested on a larger dataset nor was it automatic.

Puttonen et al. (2010) used TLS and hyperspectral data to classify 24 trees of three species with a support vector machine (SVM). The scanning was done indoors, so point cloud segmentation into trees was not required. The classification features included shape parameters computed from the TLS data and averaged reflectance values of the hyperspectral data. With a combination of 2 features from each dataset, the average classification accuracy was over 85 % for all species. When using only a pair of TLS data features, the accuracy was over 70 % for only 43 % of the pairs, but the best classification accuracy was 95.8 %.

Puttonen et al. (2011) combined mobile laser scanning (MLS) and hyperspectral data to classify 133 trees of 10 species with SVM. Individual trees were manually isolated from the point cloud. Similarly to (Puttonen et al., 2010), the classification features consisted of MLS-based shape parameters and per channel averaged spectral data. The results showed that MLS features on their own were able to separate coniferous and deciduous trees with 90.5 %, and individual species with 65.4 % accuracy. For the combination of MLS and spectra the percentages were 95.8 % and 83.5 %, respectively.

Vauhkonen et al. (2013) tested hyperspectral LiDAR (HSL) in laboratory conditions for classifying 18 spruce and pine trees. The classification accuracies varied between 78 % and 89 %. Different scans of the same trees were used for training and classification.

Othmani et al. (2013) used the 3D texture of the bark of 230 trees of five species. In their approach a 30 cm long patch is manually isolated in a stem and its texture analysed using 2D signal processing techniques and a random forest (RF) classifier. The overall species recognition was 88 %.

In the most recent study (Lin and Herold, 2016), 40 trees of 4 species were classified by using SVM and *explicit tree structure* parameters (ETS). In contrast to the shape parameters used by, e.g., (Puttonen et al., 2011), ETS parameters describe the actual shape of the tree stem or crown rather than the distribution of TLS samples. The authors refer to tree isolation details in (Holopainen et al., 2013) but fail to state which of the methods was used, and thus the level of automation is unknown. At least the separation of stem and branch points is done interactively. The classification tests were done using the leave-one-out cross-validation (LOOCV) in two different scenarios, maximum and robust, with accuracies 90.0 % and 77.5 %, respectively. The authors state that the latter scenario is more likely to be suitable for real applications.

The above literature survey shows that the tree species recognition from TLS data has been the topic of only a few studies and in most cases it has been combined with other data sources to achieve sufficient classification accuracies. Furthermore, the sample sizes have been relatively small, and no fully automatic solution has been presented yet.

In this paper we propose a proof-of-concept for fully automatic species recognition approach from TLS measurements. Rather than using 3D point cloud data directly for classification, trees are first reconstructed as quantitative structure models (QSM) (Raumonen et al., 2013; Calders et al., 2015b). Notice that the QSM reconstruction is done by using only the xyz-coordinates of the points and thus no intensity data, spectral information, photographs, or ultra-high resolution scans are required. The classification features are computed from the geometric and topological tree properties stored in the models, which means that we have more than three dimensions to work with. This enables the use of properties that have been hard or impossible to determine directly from the point cloud data. The proposed classification features are listed in Sect. 2.5.

For the species recognition, we tested three different classification methods with numerous feature sets to show their differences and suitability for the application. Namely, we tested k-nearest neighbours, multinomial regression, and support vector machine based approaches. The classification methods are presented in Sect. 2.4.

It has been shown that QSMs can be automatically computed in massive scale (Raumonen et al., 2015), and when combined with automated feature computations it makes the complete classification procedure fully automatic. To demonstrate the approach, three large, mainly single-species plots from Finland are used. In addition, two mixed-species forest plots, also from Finland, are used to demonstrate preliminary results from more heterogeneous stands. The three species

are the most numerous in Finland and represent both deciduous Silver birch (*Betula pendula* Roth) and coniferous Scots pine (*Pinus sylvestris* L.) and Norway spruce (*Picea abies* [L.] Karsten). Forest plot and scanning setup details are presented in Sect. 2.1 and 2.2, respectively. We present results in Sect. 3, and sum up in Sect. 5.

2 Materials and methods

2.1 The forest plots used for the demonstration

We have three large almost single-species forest plots and two unmanaged mixed-species stands, which have been scanned with TLS. One of the single-species plots is a systemically planted plot with only Silver birch trees and the other two are natural coniferous plots with Norway spruce and Scots pine trees. All three study plots are in Punkaharju, Finland, where annual mean precipitation is 600 mm and effective temperature sum 1300 dd (Merilä et al., 2014).

Silver birch plot

A Silver birch stand used in this study is a field experiment in Punkaharju, Finland ($61°48'$N, $29°18'$E), established in 1999 to study within-stand differences among genotypes (22 genotypes micropropagated from local trees) (Possen et al., 2014). Trees were planted on agricultural field with a planting distance of 2×2 m in 1999. In April 2008, 50 % of the trees were harvested. At the time of the scanning in October 2014, the stand density was approximately 1000 trees per ha, height of the trees varied from 18 to 24 m, and diameter at the height of 1.3 m (DBH) was 10–17 cm.

Scots pine plot

The Scots pine dominated study plot in Punkaharju, Finland ($61°46'$N, $29°20'$E) is conventionally managed forest. The latest thinning took place in 1994, thereafter only dead trees are removed. At the time of the TLS in October 2014, the stand age was 95 years, stem number was approximately 500 stems per ha, the DBH was 18–40 cm, and the height of trees 27–32 m. The stand grows on sub-xeric site and the average stem volume growth is 11 m^{3}ha^{-1}yr^{-1}. Scots pine and Norway spruce dominated study plots belong to the European forest monitoring network established under the UN-ECE ICP programme (Derome et al., 2002; Merilä et al., 2014).

Norway spruce plot

The Norway spruce dominated stand of this study is conventionally managed forest on herb-rich site, where the latest thinning took place in 1994 and since then the site has been a part of forest monitoring programme. The stand is located in Punkaharju, Finland and the density was approximately 400 stems per ha, the DBH was 28–45 cm, and the height of trees 28–33 m. The average stem volume growth is 8.8 m^{3}ha^{-1}yr^{-1} (Merilä et al., 2014).

Mixed-species plots

The two mixed-species plots are located in Sipoo ($60°28'$N, $25°12'$E) and Lapinjärvi ($60°39'$N, $26°7'$E) in Southern Finland. These sites are unmanaged Norway spruce dominated forests (>70 % of standing volume), where other tree species were also present. At the time of the scanning in 2014, the stand density was approximately 1300 trees per ha in Sipoo and 1000 trees per ha in Lapinjärvi. For further details see (Rajala et al., 2012).

2.2 Terrestrial laser scanning

The scanning of all forest plots was performed with a RIEGL VZ-400 scanner and a 0.04 degree resolution. The Silver birch (leaf-off) and Scots pine plots were scanned completely on October 21st, 2014. The scanning of the Norway spruce plot was started on the same day and completed on November 26th, 2014. On both days the weather was cloudy with no rain and light wind, and the temperatures were $-1°$C and $+1°$C, respectively. The approximate scanning times were 1, 3 and 4 (2+2) hours for the Silver birch, Scots pine and Norway spruce plots, respectively. The Sipoo plot was scanned on November 20th, 2014 and Lapinjärvi plot on November 24th, 2014. On both days the temperature was close to $0°$C. The number of scanning points per forest plot was selected during the measurements based on visibility in order to cover most of the trees in the scans.

Retroreflectors were attached to tree stems to enable co-registration, which was later performed with the RiScan Pro software. The number of points in the scans, initially and after plot restriction and filtering, were the following: 94 and 35 million for the Silver birch plot, 300 and 58 million for the Scots pine plot, and 340 and 116 million for the Norway spruce plot. For Sipoo and Lapinjärvi the filtered point counts were 126 and 105 million, respectively. Stem locations and tree heights for each of the study plots are presented in Fig. 1, together with the scanner locations.

## 2.3 Tree extraction and quantitative structure models

The individual trees were automatically extracted from the point clouds, but only in a suitable region close to the scanners. The extraction method was similar to the one presented in (Raumonen et al., 2015). In the extraction process the point cloud is first filtered for noisy measurements and isolated points that should not contribute to the reconstruction process, and the local ground level is estimated. The filtered point cloud is then partitioned into small subsets or surface patches about $10-20$ cm in diameter. These patches are the smallest parts used for tree segmentation. The principal components of the patches are then used to locate the stems based on simple heuristics about the stems being vertical. Next the located stems are taken as initial sets for the trees and the stems are expanded using surface growing (using the neighbour relation of the patches). There will be separate components that cannot be reached from any tree by surface growing and these components are then connected to the closest point in the closest expanded tree. At this point most of the trees are uniquely separated except in some cases where the initially expanded stems are connected. The final separation is then achieved with the segmentation of the point cloud into stems and branches. The segmentation follows the procedure presented in (Calders et al., 2015b; Raumonen et al., 2015).

The tree extraction process is prone to some minor errors, and occasional larger errors when some trees are very close to each other and their crowns are occupying the same space. However, the errors in the separation occur mostly in the top parts of the tree crowns, where there is also typically low point cloud coverage due to the extreme angle of the scanner and occlusion. The separation errors most often manifest as a set of branches of a tree incorrectly being contributed as a part of one of its neighbouring tree. An example of this can be seen in Fig. 2. Due to the possibility of such errors, the species classification features were selected to be insensitive in this regard. The features utilize parts of the trees that are expected to be reconstructed most accurately, e.g., branches that originate from the stem. Furthermore, the crown radius, a property that is key to many of the features, is estimated from the volume distribution of the cylinders, rather than their absolute positions, making the estimate more robust should the crown contain parts of the neighbouring trees.

As a result of the tree extraction, the point cloud is partitioned into subsets that represent single trees. These subset point clouds are used for the reconstruction of QSMs of the individual trees one-by-one. For each tree, the QSM reconstruction process creates another partition of the tree point cloud into small patches, and then segments them into the stem and branches. This new partition utilizes the first segmentation from the tree extraction step to determine a finer and variable-size partition of the tree point clouds. The size of the patches in the partition is determined based on the branching structure and branch size estimates. Next the patches are segmented into the stem and individual branches similarly as earlier. After the segmentation a cylindrical QSM is reconstructed by fitting cylinders into the segments.

All the QSMs were reconstructed with the same input parameters: the minimum and maximum patch diameters were 3 cm and 12 cm and the relative cylinder length (length/radius) was 5. The parameter values were selected based on previous studies with QSMs to have reasonable models with short computation time (few minutes per tree). Thus the QSMs used in this study were not optimized to be the best possible ones. The optimization of the QSMs could be based on, e.g., median point-to-model distances, as shown in (Hackenberg et al., 2015), but that would require even tens of models per tree and thus equivalent increase in computation time. However, one could try a compromise between these two opposites: A reasonable assumption is that the trees and the quality of the measurement data (resolution, noise level, occlusion, etc.) are similar inside the plot. Therefore at first few trees could be selected for parameter optimization and then use the optimum parameters for all trees.
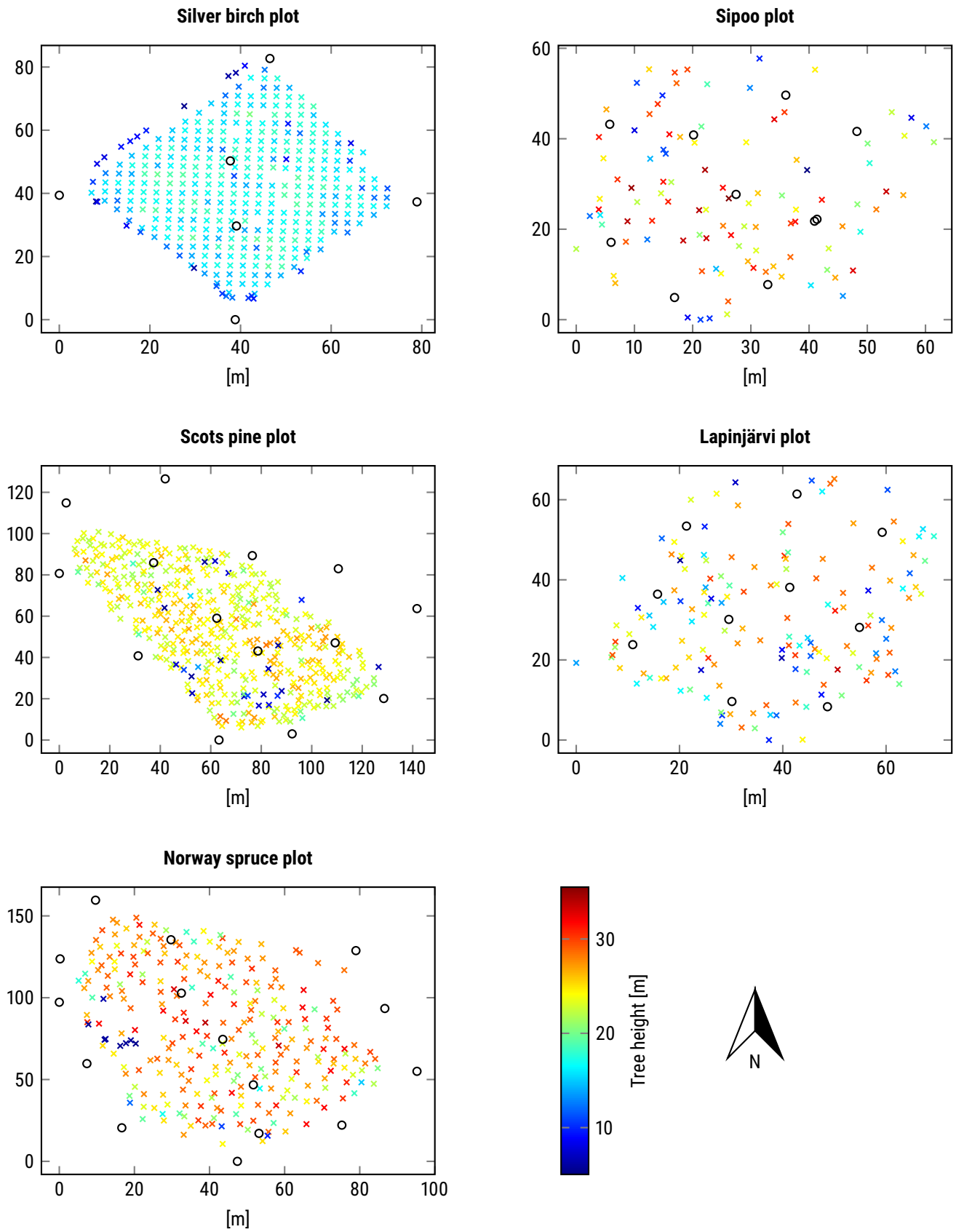
Figure 1: Forest plot tree location and height map (crosses) and scanner positions (circles). The height colour scale is the same for all plots.

Side	Top
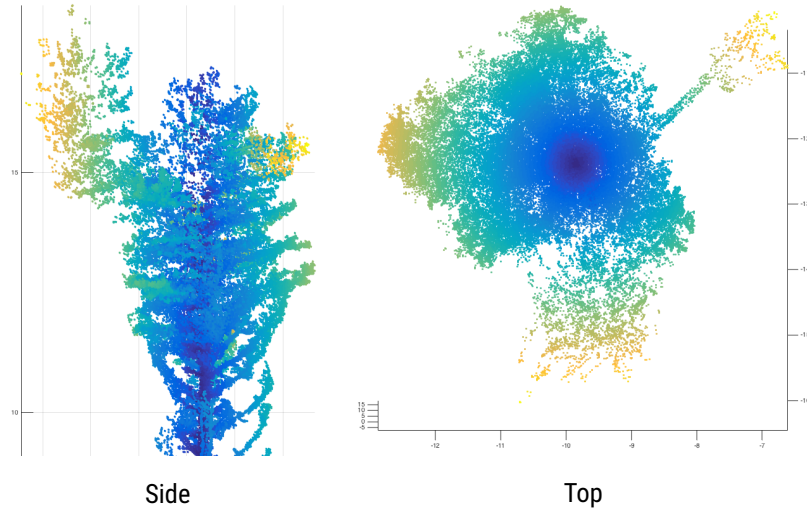
Figure 2: Example error in tree extraction in on of the Scots Pines. Parts of the crown of a neighbouring tree have been contributed to the tree in error.

2.4 Classification methods

In this section we outline classification methods that are used to classify trees into tree species based on selected *features*, that are defined in Sect. 2.5. Given M features and K species labels, a training set *TEACH* is a set of pairs $(\mathbf{x}, species)$, where $\mathbf{x} \in \mathbb{R}^M$ is a list of feature values and $species \in SPECIES = \{species_1, species_2, \ldots, species_K\}$. Either by using the training data, or a model derived from it, the classification methods are able to assign the elements of a test set $TEST = \{\mathbf{x}_i\} \subset \mathbb{R}^M$ into one of the K species classes in *SPECIES*. All the presented methods are also able to present probabilities p_{ij} for an element $\mathbf{x}_i \in TEST$ to belong to a class $species_j \in SPECIES$. Thus, a classification method produces a result set of pairs $(\mathbf{x}_i, \mathbf{p}_i)$, where $\mathbf{x}_i \in TEST$, $\mathbf{p}_i = (p_{i,1}, \ldots, p_{i,K})$, $p_{ij} \in [0,1]$ and $j \in SPECIES$. The resulting assigned class for a test element $\mathbf{x}_i$ is defined as the class j with the maximum probability p_{ij}.

2.4.1 k-nearest neighbours

The k-nearest neighbours algorithm finds the k elements from the training set *TEACH* that are the closest to a test point $\mathbf{x}_i \in TEST$. The class probability p_{ij} of the element $\mathbf{x}_i$ is defined as the relative number of elements with class j belonging to the subset of k nearest neighbours. Various distance measures can be used when finding the closest elements.

On the implementation level, the `knnsearch` function bundled in MATLAB was used for this classification method. Number of neighbours parameter k and the distance measure were optimized during computations.

2.4.2 Multinomial regression

For classification based on multinomial regression the `mnrfit` and `mnrval` commands part of the Statistics and Machine Learning Toolbox in MATLAB were used. In a multinomial logistic regression model the probability p_{ij} of a sample $\mathbf{x}_i \in TEST$ having class $species_j \in SPECIES$ can be computed as (Agresti, 1990, p. 313):

$$p_{ij} = \frac{\exp\left(\mathbf{x}_i^{\mathsf{T}} \mathbf{b}_k\right)}{\sum_{k=1}^{K} \exp\left(\mathbf{x}_i^{\mathsf{T}} \mathbf{b}_k\right)}. \tag{1}$$

For a selected baseline class (*e.g.* $j = K$) the coefficients $\mathbf{b}_j$ are set to zero, and for the rest of the classes the coefficients are optimized in an iterative fitting process with the *TEACH* data set. The predicted outcome class is defined to be the one with the highest probability.

2.4.3 Support vector machine

Support vector machine classification finds a hyperplane that maximizes the margin between the samples of two different classes. In a two-class case the optimization problem can be formulated as a minimization problem as follows:

$$\min_{\mathbf{w}, \xi, b} \frac{1}{2} K(\mathbf{w}, \mathbf{w}) + C \sum_{i=1}^{l} \xi_i, \tag{2}$$

subject to

$$y_i \left(K(\mathbf{w}, \mathbf{x}_i) - b\right) \geq 1 - \xi_i \tag{3}$$
$$\xi_i \geq 0, \tag{4}$$

where $\mathbf{w}$ is the normal vector of the hyperplane and b the plane's location parameter, and C is the penalty parameter. In a two-class case the class indicator y_i of the sample $\mathbf{x}_i$ is 1 if the sample has the class i and -1 otherwise. Furthermore, ξ_i are the slack parameters for a soft margin to allow the overlap of classes. The $K(\cdot, \cdot)$ function is called the kernel function which defines the shape of the class boundary. By using the *linear* kernel function

$$K(\mathbf{a}, \mathbf{b}) = \mathbf{a}^T \mathbf{b}, \quad \mathbf{a}, \mathbf{b} \in \mathbb{R}^M \tag{5}$$

the boundaries are hyperplanes. Other kernel functions used in this study are *polynomial* and *radial basis function* (RBF), respectively:

$$K\left(\mathbf{a}, \mathbf{b}\right) = \left(\gamma \mathbf{a}^T \mathbf{b}\right)^d \tag{6}$$

$$K\left(\mathbf{a}, \mathbf{b}\right) = e^{-\gamma \|\mathbf{a} - \mathbf{b}\|^2}, \tag{7}$$

where γ and d are kernel parameters. The use of these additional kernel functions allows the decision boundaries to be non-flat. Support vector machine based classification with a linear, polynomial, and RBF kernel functions are noted as SVM$_{\text{lin}}$, SVM$_{\text{pol}}$, and SVM$_{\text{rbf}}$, respectively. For $K > 2$ species classes the classifier can be implemented in $K - 1$ steps, where on the kth step the two possible classes are *species$_k$* and *SPECIES \ species$_k$*. The `libsvm` package (Chang and Lin, 2011) for MATLAB was used for the computations. Grid search was used for finding the optimal values for the penalty parameter C and the kernel parameters γ and d.

2.5   Tree features

All the classification methods presented in Sect. 2.4 are based on feature data. In this study each feature is a scalar value computed for a single tree (QSM). The features are derived from the geometric and topological properties stored in the reconstructed QSMs. The features were designed to be scale-independent by scaling absolute lengths with, e.g., the tree height or DBH. By using such features the classification should perform well with both young and old trees. Table 1 lists the features that were used in this study. Apart from Features 1, 11 and 14, the features are unitless. Additionally, the Classification features -animation shows how the features are defined and computed. In the animation a single Scots pine model is used to illustrate the features one-by-one (See Supplementary Data).

Stem branches (SB) are first-order branches that originate from the stem. The branching angle was computed as the angle between the axes of the first cylinder in the branch and its parent cylinder. The branching cluster size, Feature 2, was approximated by inspecting the start points of the SBs. An inspection height interval with a width of 40 cm was centred at the height of each SB. The number of SBs inside the interval was recorded and the branches were flagged as *used*. Only the SBs without the *used* flag were computed, thus allowing any branch to be part of only one branching cluster; *i.e.*, height interval. At the end, the cluster sizes were averaged for every tree.

DBH was computed by fitting a cylinder at the standard height to the stem point cloud during the reconstruction process and stored in the tree model. The SB radius, Feature 3, was defined to be the average ratio between the radii of the SBs and their respective parent cylinders. Only ten SBs with the largest radius at their base were selected for this feature to get a better separation between species.

Using the topological information stored in a cylinder model the set of crown cylinders was found, using the following algorithm, that is designed to exclude dead branches at the bottom of the stem:

1. Initialize the crown set as cylinders that have a branching order higher than three. If the initial set is empty, the minimum order is lowered until the set becomes non-empty.

2. As long as the crown set extends, append the parent cylinders of the crown set that are not part of the stem.

3. Append to the crown set cylinders that are not part of the stem but whose start point is higher than the lowest starting point of crown cylinders connected to the stem.

4. As long as the crown set extends, append the child cylinders of the crown set.

The initial crown height is defined as the relative starting height of the lowest SB in the crown. The crown height is the difference between the lowest and highest crown cylinders normalized by the tree height. To analyse how evenly the crown bottom is distributed, the crown set is divided into eight angular bins around the stem, and the minimum vertical point is computed. The crown evenness feature is the ratio between the highest and lowest of these values.

Features 9 and 12 require an estimate of either the tree or the crown radius. Rather than computing the radius estimate directly from the positions of the cylinders furthest from the stem, we use a radial volume distribution for robustness. To estimate the tree radius at different heights, a tree is divided into three vertical bins, and the centre point of each bin is defined as the average of mean points of stem cylinders in the bin. If the bin does not contain stem cylinders the centre of the previous bin is used. The tree radius estimate in a vertical bin is defined as the radius of a cylinder whose axis is vertical and goes through the bin centre point, and which contains 90 % of the volume of the cylinders in that bin. The crown diameter is estimated as two times the maximum vertical bin radius.

For Feature 13 the branch cylinder volume distribution is considered in the vertical direction. A good vertical limit 55 % of the total tree height was found by testing numerous alternatives. For Feature 15 only the bottom third is considered as it is expected to contain most of the dead/shed branches, which are defined as branches without child branches.

To see the value range and the level of separation between species for the proposed features Fig. 3 visualizes the distribution of each feature per species. The Species separation -animation also shows the distribution of feature values per species, together with an example model of each species and the respective feature values of these models (See Supplementary Data). Furthermore, Fig. 4 visualizes the two-dimensional feature space of Features 1 (stem branch angle) and 13 (volume below 55 % of height). Three individual QSMs are also shown and their mapped values in the selected feature space highlighted. The values in both figures were computed using the full population of 358 Silver birch, 457 Scots pine, and 276 Norway spruce trees from the three single-species forest plots.

3   Results

In this section we first use the three single-species Punkaharju plots for three different purposes: First we optimise the
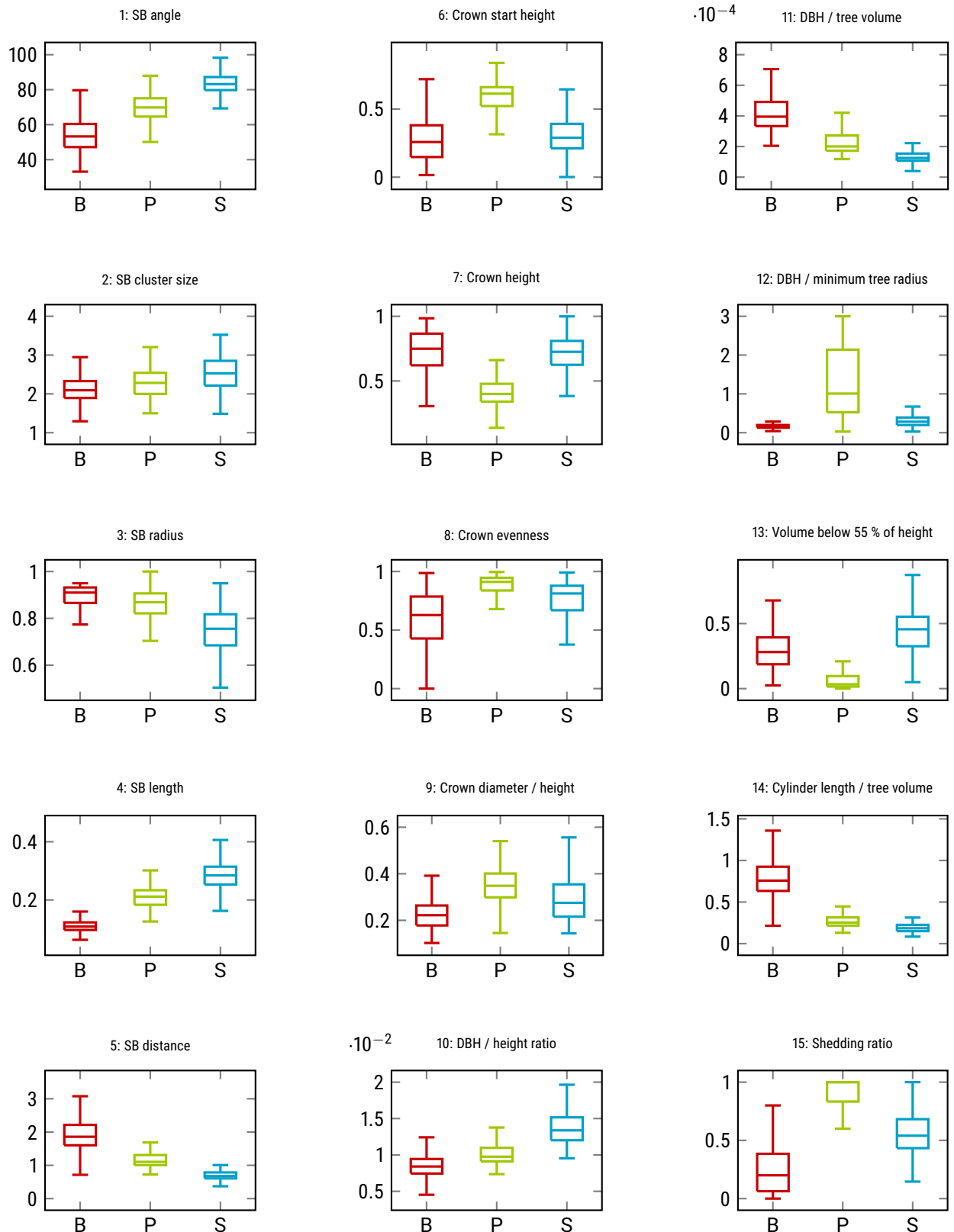
Figure 3: Box plots of classification features for each tree species: Silver birch (B), Scots pine (P) and Norway spruce (S). The vertical line inside the box is the median. Box limits give the 1st and 3rd quartiles of the distribution and the whiskers extend to 1.5 times the distance between the 1st and 3rd quartiles, or the distribution extremes.

Table 1: List of included tree classification features. Possible units are given in brackets.

	ID	Feature name	Description
Stem branch	1	Stem branch angle	Median of the branching angles of the 1st order branches in degrees. 0 is upwards and 180 downwards. [°]
	2	Stem branch cluster size	Average number of 1st order branches inside a 40 cm height interval for 1st order branches. Each branch can only belong to one interval.
	3	Stem branch radius	Mean ratio between the 10 largest 1st order branches measured at the base and the stem radius at respective height.
	4	Stem branch length	Average length of 1st order branches normalized by DBH.
	5	Stem branch distance	Average distance between 1st order branches computed using a moving average with a window width 1 m. If window is empty average distance in window is set as half of window width.
Crown	6	Crown start height	Height of first stem branch in tree crown relative to tree height.
	7	Crown height	Vertical distance between the highest and lowest crown cylinder relative to tree height.
	8	Crown evenness	Crown cylinders divided into 8 angular bins. Ratio between extreme minimum heights in bins.
	9	Crown diameter / height	Ratio between crown diameter and height.
Tree	10	DBH / height ratio	Ratio between DBH and total tree height.
	11	DBH / tree volume	Ratio between DBH and total tree volume. $[m^{-2}]$
	12	DBH / minimum tree radius	Ratio between DBH and the minimum of the vertical bin radius estimates.
	13	Volume below 55 % of height	Relative cylinder volume below 55 % of tree height.
	14	Cylinder length / tree volume	Ratio between total length of all cylinders and total tree volume. $[m^{-2}]$
	15	Shedding ratio	The number of branches without children divided by the number of all branches in the bottom third.
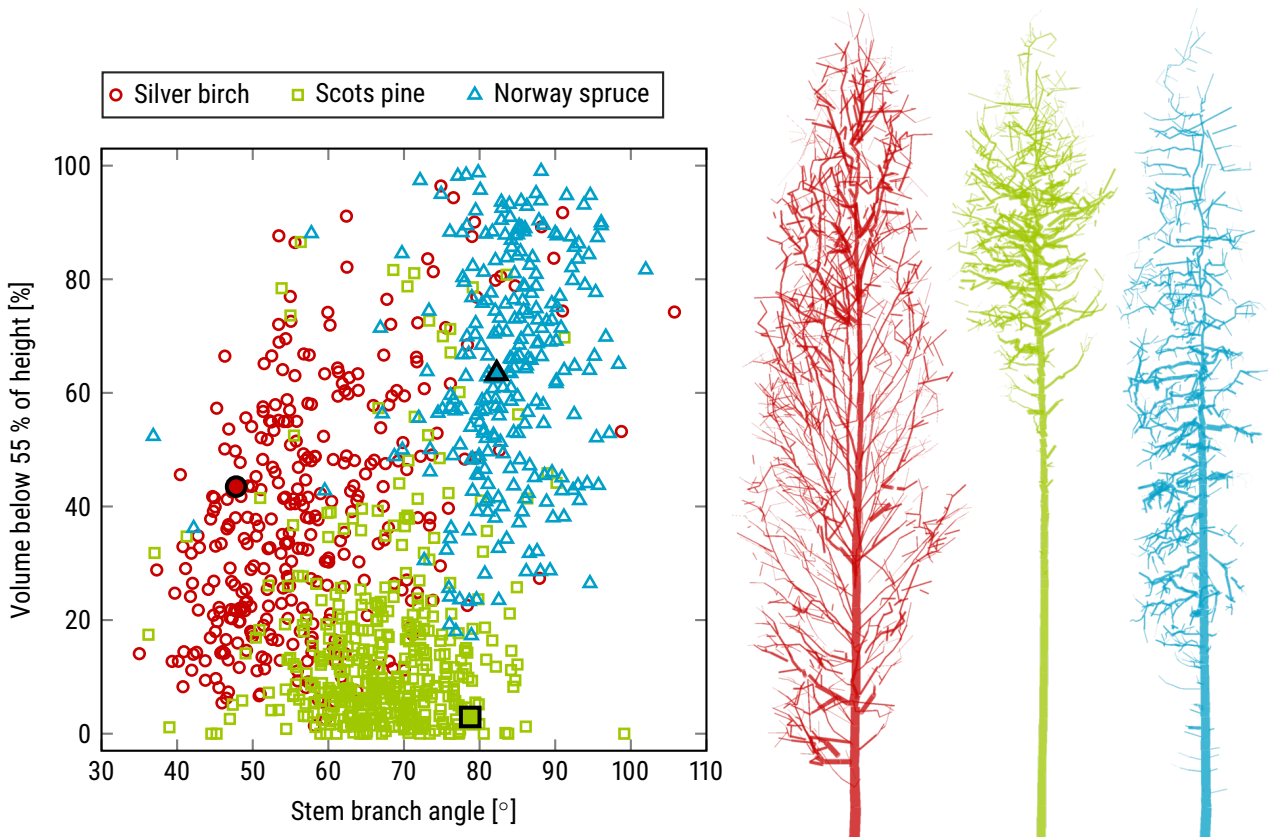
Figure 4: Example QSMs and feature distribution for Features 1 and 13. The highlighted markers in the distribution correspond to the colour-coded models.

Table 2: Limits and results for SVM kernel parameters γ^* and d, and the penalty parameter C^* grid search.

	C^*	γ^*	d
Minimum	-5	-15	2
Maximum	15	3	5
Increment	1	1	1
Optimums			
linear	-2	-	-
polynomial	-5	2	2
RBF	1	-3	-

parameters of the classification methods, then we determine the optimal feature sets, and finally we study the effect of the size of the training data set. In Sect. 3.4 we test the classification performance of the optimal parameters and feature sets on mixed-species forest plots, both by using only the single-species plots as training data, and by supplementing the training data with samples from the mixed-species plots.

3.1 Optimal parameters

The parameters of the k-NN method were optimized by using 50 samples of each species and 10-fold cross-validation. The value of k was varied from 2 to 20 and the distance measure in the following parameter set: `euclidean`, `seuclidean`, `cityblock`, `chebychev`, `minkowski`, `mahalanobis`, `cosine`, `correlation`, and `spearman`.

The highest classification accuracy was achieved with $k = 4$ and the standardized Euclidean distance (`seuclidean`). This combination of parameters was used in all following tests, and is noted as 4-NN.

In order to find the optimal SVM kernel and penalty parameters, a grid search was performed for all of the kernel types. The following convenience parameters were defined for the grid search:

$$C^* = \log_2 C \tag{8}$$
$$\gamma^* = \log_2 \gamma. \tag{9}$$

The grid search was performed on the same 50 samples of each tree species, and was carried out using 5-fold cross-validation provided by the `libsvm` package. The grid limits and results for the search are presented in Table 2. The parameters that yielded the highest classification accuracy were fixed for further classification tests for each kernel type.

3.2 Optimal feature sets

To find the optimal classification features, the included feature count was varied from 1 to 15. For each feature count all the possible feature combinations were tested using a 10-fold cross-validation. The remaining trees of each species after the parameter optimization were divided into ten subsets of equal size. Each subset was then classified by using the remaining nine subsets of each species as training data. The 10-fold cross validation was selected to show the classification

performance in close to optimal conditions, where the amount of the training data far exceeds the amount of the test data. The maximum classification accuracies for each method and feature count are listed in Table 3.

When using just one feature, the maximum classification accuracy, 85.3 %, was achieved with the 4-NN method and Feature 5: Stem branch distance. This combination was able to separate Silver birches and Norway spruce trees from each other but mixed birches with Scots pines, as 12.4 % of birches were misidentified as pines and 15.1 % *vice versa*.

When the feature count was two, the 4-NN and SVM$_{\text{lin}}$ classification methods gave the maximum accuracy with Features 5 and 12. The values of these features are visualized in Fig. 5 to show the high level of species separation. For the remaining three methods, the best combination was Features 11 and 15. The maximum total accuracy, 92.0 %, was received with the 4-NN method. With this configuration the standard deviation over the folds was 1.4 pp. and the biggest confusion was again between birches and pines.

For feature counts higher than two there is no clear difference between the methods as the standard deviation of the classification accuracies over the methods remain between 1.23 and 2.89 percentage points. With feature counts from 6 to 15 all the methods result in accuracies above 93.0 %.

The highest accuracy, 96.9 %, was obtained with the 4-NN method and 10 features. The resulting relative and absolute confusion tables are presented in Table 4. The results show that out of 1010 trees only 31 were misclassified when using this setup.

For further testing, *top feature sets* were selected using the following two criteria: 1) sets whose average classification accuracy over the methods was above 95 %; 2) sets whose minimum classification accuracy over the methods was above 94 %. 120 combinations fulfilled the first condition, and 16 combinations the second. Out of these combinations, ten fulfilled both and these combinations are listed in Table 5.

Fig. 6 shows the frequency at which each feature is part of the 126 top feature sets. Out of the 15 features, four (1, 10, 13, 14) are part of all the top feature sets. Next the top feature sets are used for testing the effect of training data size.

The independence level of the classification features was tested by studying the covariance of the features over the total population of 1010 trees. The correlation between Features 6 and 7 is over 99 % because none of the included species have crowns that extend below the lowest connecting stem branch. Furthermore, Features 4 and 11 have a correlation over 80 %. The connection here is not that obvious as Feature 4 measures stem branch length and Feature 11 total volume of the tree. The correlation is expected to drop for both feature pairs when additional species with varying geometry are included. For the purpose of this study the high correlation between these pairs did not affect the classification accuracies, as is evident from the similar results with feature combinations containing and not containing the highly correlated feature pairs, *e.g.*, in Table 5.

Table 3: Classification accuracy $\overline{p}$ in percentages and standard deviation σ for cross-validation in percentage points for best feature combinations with increasing feature count. The highest accuracy for each count is highlighted, and the total maximum value is underlined.

| Feat. count	4-**NN** $\overline{p}$	σ	**MNR** $\overline{p}$	σ	**SVM**$_{lin}$ $\overline{p}$	σ	**SVM**$_{pol}$ $\overline{p}$	σ	**SVM**$_{rbf}$ $\overline{p}$	σ
1	**85.3**	3.0	76.7	3.0	80.7	3.0	84.6	3.0	81.1	3.0
2	**92.0**	1.4	89.8	2.8	88.8	1.4	90.6	2.8	90.1	2.8
3	**94.6**	1.3	91.5	2.8	91.2	2.6	92.7	2.4	92.3	1.9
4	**95.4**	1.3	92.5	2.1	92.7	2.1	94.7	2.0	93.8	2.0
5	**96.1**	2.2	93.0	2.6	93.6	1.7	95.4	1.7	94.9	1.7
6	**96.2**	1.5	93.6	2.0	93.6	1.7	95.8	2.9	95.1	1.7
7	**96.8**	1.9	93.8	1.2	93.8	1.8	96.2	1.8	95.5	2.0
8	**96.6**	1.8	94.2	2.6	94.1	2.1	96.4	1.8	95.5	1.8
9	**96.8**	1.6	94.2	2.7	94.4	2.4	96.4	2.4	95.8	2.2
10	<u>**96.9**</u>	2.1	94.3	2.1	94.5	2.2	96.7	1.9	95.8	1.8
11	96.6	1.5	94.4	2.3	94.6	1.9	**96.8**	1.9	95.9	1.5
12	**96.7**	1.2	94.5	1.8	94.3	2.2	**96.7**	2.0	95.9	1.8
13	**96.5**	1.8	94.4	2.1	94.2	2.8	96.3	2.2	95.9	2.1
14	**96.4**	1.6	94.6	2.2	94.4	1.7	96.1	1.6	95.8	1.7
15	**96.1**	1.8	93.9	1.8	94.1	1.8	95.5	1.8	95.7	1.8
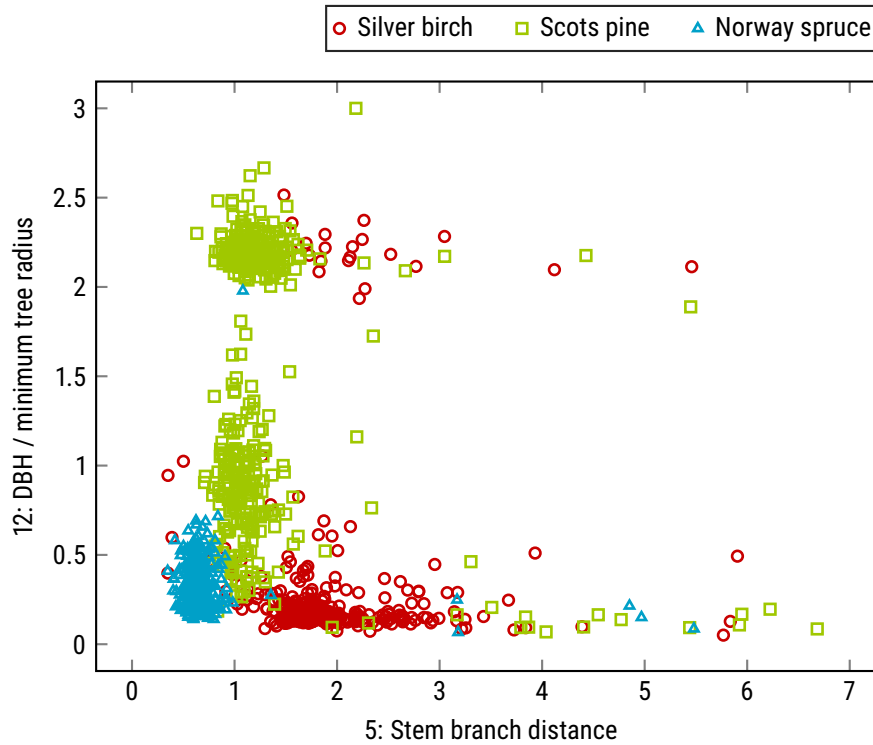
Figure 5: Data separation with the feature pair that produced the maximum classification accuracy with the 4-NN and SVM$_{lin}$ methods.

Table 4: Relative and absolute confusion tables for 4-NN method and 10 features with highest classification accuracy.

		Predicted					
		B	P	S	B	P	S
	Silver birch	**98.2**	1.5	0.3	**324**	5	1
Correct	Scots pine	3.0	**96.3**	0.7	13	**414**	3
	Norway spruce	1.6	2.0	**96.4**	4	5	**241**
		Relative			Absolute		

Table 5: Top feature sets that fulfilled both conditions with their classification accuracy per method and averaged in percentages. The maximum accuracy over the listed feature sets is highlighted for each method.

#	Feature set	4-NN	MNR	SVM$_{lin}$	SVM$_{pol}$	SVM$_{rbf}$	Average
1	1, 2, 3, 5, 7,10,11,13,14,15	96.2	94.1	94.2	96.1	95.5	95.2
2	1, 2, 3, 5, 8,10,11,12,13,14	96.2	94.3	**94.5**	**96.2**	95.4	95.3
3	1, 2, 3, 6, 8,10,11,13,14,15	96.1	94.3	94.3	95.2	95.5	95.1
4	1, 2, 3, 7, 8,10,11,13,14,15	96.0	94.3	94.3	95.2	95.4	95.0
5	1, 2, 3, 5, 6, 8,10,11,12,13,14	**96.4**	94.1	94.1	96.0	95.3	95.2
6	1, 2, 3, 5, 6, 7, 8,10,11,13,14,15	95.8	94.2	94.1	95.8	95.8	95.1
7	1, 2, 3, 5, 6, 7, 8, 9,10,11,13,14,15	96.1	94.4	94.1	95.8	**95.9**	95.3
8	1, 2, 3, 5, 6, 7, 9,10,11,12,13,14,15	96.0	94.3	94.2	95.5	95.7	95.1
9	1, 2, 3, 4, 5, 6, 7, 8, 9,10,11,13,14,15	96.2	94.2	94.4	95.6	95.8	95.2
10	1, 2, 3, 5, 6, 7, 8, 9,10,11,12,13,14,15	96.2	**94.6**	94.1	95.3	95.7	95.2
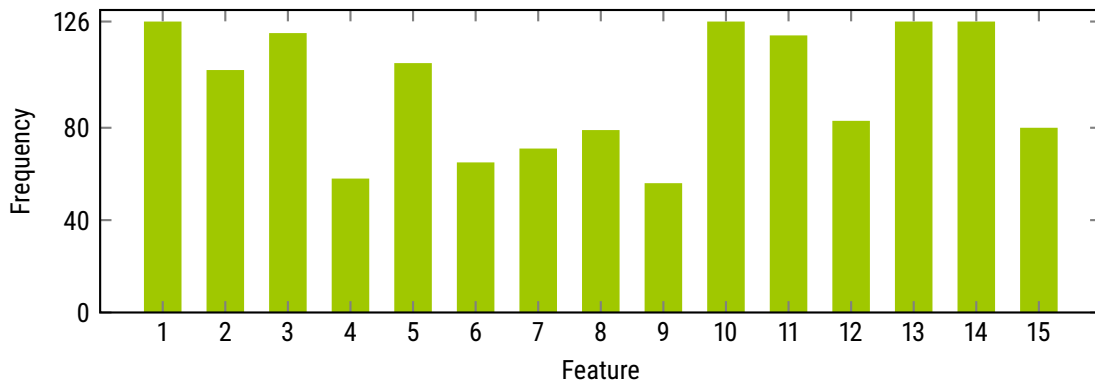
Figure 6: Number of times a feature was part of the 126 top feature sets.

3.3 Effect of the size of training data set

In order to test how each of the proposed classification methods performs in real applications, the effect of the amount of training data was studied. The number of trees per species in the training data set was varied from 4 to 150, while the same number for the testing data remained constant at 50. The tree samples were selected randomly from the complete tree population, but the training and testing sets remained disjoint. Sampling was repeated 10 times for each training data size. The optimal parameters from Sect. 3.1 were used in the test, as well as, the top feature sets from Table 5.

Table 6 shows the total classification accuracy of each method as a function of the amount of training data. The accuracy of a method is averaged over the random repeats and the feature combinations. Furthermore, Fig. 7 shows the average, minimum and maximum classification accuracies for the same data.

The 4-NN method has the highest average classification accuracy and the lowest standard deviation with all training data sizes. With data sizes above or equal to 30, the average classification accuracy remains above 93 %, and the minimum accuracy above 88 %. The MNR and SVM$_{lin}$ methods also perform well with an average accuracy above 91 % with 50 samples or more. The standard deviation is a little greater than with the 4-NN method but the minimum classification accuracies still remain above 82 %, and with a high number of samples (≥ 100) even comes near 87 %.

The SVM$_{pol}$ and SVM$_{rbf}$ methods have relatively hight standard deviation with all sample sizes but still below 4 pp. The average accuracy on the SVM$_{pol}$ method is very good, but some of top feature sets give poor results dropping the minimum performance quite low, even with a high number of training samples. Similarly, the SVM$_{rbf}$ method has a relatively low minimum performance, but unlike with the SVM$_{pol}$ method, the effect seems to diminish with the increasing number of samples. For operational use the 4-NN, MNR and SVM$_{lin}$ methods seem to provide the most consistent results.

While performing the accuracy testing described above, the correlation between tree properties, the measurement setup, and the probability of an incorrect classification was studied. As the tree sets were randomly sampled, the number of picks per tree was stored, as was the number of incorrect classifications. The probability of incorrect classification was computed as the ratio between the two numbers. The results showed that there was no correlation between the probability to be incorrectly classified and the minimum distance to the laser scanner position. Furthermore, there was no correlation between the probability and estimated tree radius, tree height, and average distance to the laser scanner position.

3.4 Performance on a mixed species forest plots

Above we used only single-species plots for training and testing. Arguably one can ask how well these results generalise to mixed-species forest, which may allow more variability for

Table 6: Average classification accuracy and standard deviation as a function of training data size per species. The average in percentages and the std in percentage points are computed over the 126 top feature sets and the 10 repeats with random data.

Sample size	4-NN $\overline{p}$	σ	MNR $\overline{p}$	σ	SVM$_{lin}$ $\overline{p}$	σ	SVM$_{pol}$ $\overline{p}$	σ	SVM$_{rbf}$ $\overline{p}$	σ
4	87.8	7.4	55.1	17.1	60.4	25.0	68.7	19.1	43.5	24.1
10	92.1	2.4	88.0	4.6	87.6	4.0	88.2	3.3	71.6	11.6
20	92.9	1.4	89.1	2.8	90.1	2.2	89.6	2.4	82.5	3.7
30	93.0	1.4	90.2	2.6	90.1	2.2	89.7	2.4	85.9	2.9
40	93.3	1.4	90.9	2.4	91.1	2.2	90.7	2.8	86.8	3.0
50	93.7	1.5	91.1	2.1	91.5	2.1	91.0	3.0	87.2	3.6
60	94.2	1.5	91.5	1.9	91.7	1.9	91.4	2.8	88.1	3.4
70	94.1	1.5	91.5	1.6	91.7	2.0	91.2	3.4	88.3	2.9
80	94.1	1.4	91.7	1.6	91.7	1.9	91.9	3.6	88.6	2.9
90	94.0	1.1	91.4	1.7	91.4	1.7	92.0	3.4	89.2	3.3
100	94.5	1.3	91.3	1.6	91.6	2.0	92.4	3.1	89.8	2.9
110	94.6	1.2	91.6	1.4	91.8	1.8	92.7	3.2	89.4	2.8
120	94.6	1.3	91.7	1.5	91.7	2.0	92.8	3.4	89.6	2.7
130	94.5	1.2	91.8	1.6	92.0	1.8	93.2	2.8	89.9	2.9
140	94.7	1.3	91.9	1.7	92.0	1.9	93.2	3.2	89.7	2.8
150	94.6	1.2	91.9	1.7	92.1	1.8	93.3	3.4	90.4	2.2
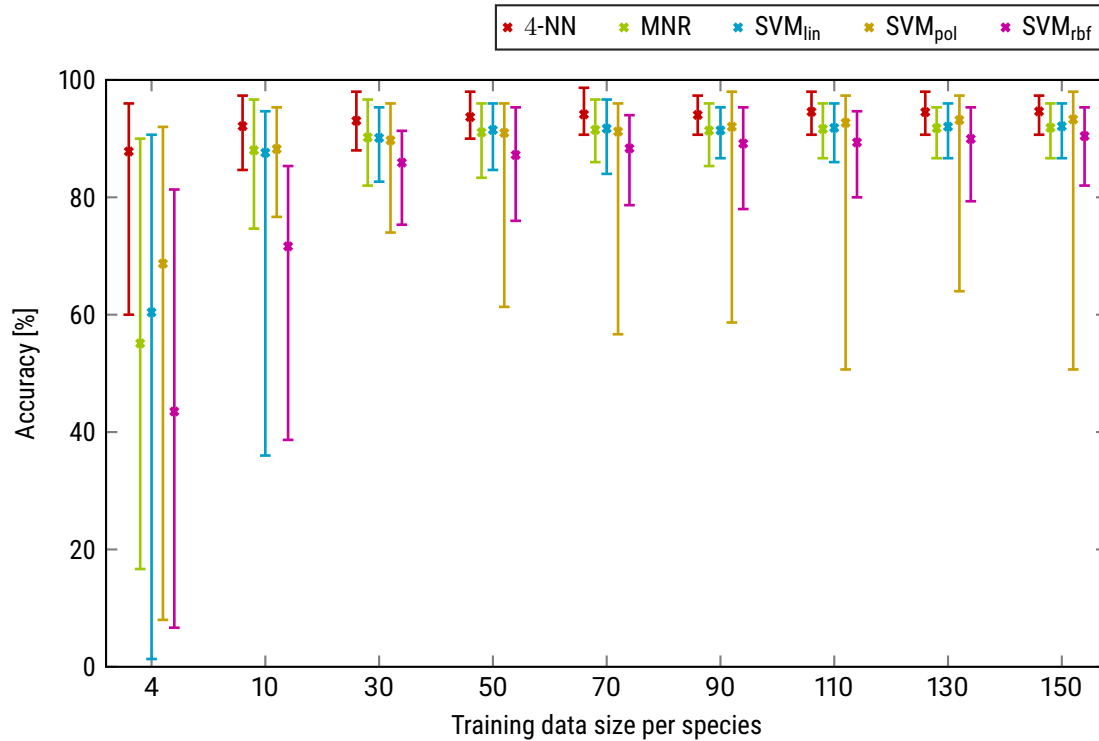
Figure 7: Average, minimum and maximum classification accuracy with changing training data size per species.

tree structures. We only have limited data for this kind of testing, and therefore, we did not use it in the above analysis. To show preliminary results we used two mixed-species plots located in Sipoo and Lapinjärvi. The forests are dominated by Norway spruce trees, but also contains Silver birches and Scots pines among other species. However, as up-to-date tree maps were not available, we manually classified the trees by inspecting point clouds of individual trees and by referencing field-measured tree maps from 2009. We identified 22 Silver birches, 13 Scots pines and 214 Norway spruce trees which were then used for testing.

Training data was sampled randomly from the Punkaharju plots, 100 trees per species. Classification accuracy was tested with all the classification methods with the optimal parameter values and the best feature combinations determined for the three Punkaharju plots listed in Sect. 3.2. Additionally, training data sampling was repeated 100 times. An additional test was performed where 100 of the Norway spruce trees from the mixed-species plots were used for training and the remaining 114 were tested, while other parameters remained the same. The other two species did not have enough samples to split them into training and testing sets. Table 7 lists the average and maximum classification results for each of the methods per tree species as well as a total accuracy for both training data sources.

When using training data from only the single-species plots the average classification accuracy is between 50 % and 55 % and the maximum around 70 %. The best result, 76.3 %, is produced with MNR method. When including Norway spruce tree samples from the mixed-species plot in the training data, all of the average and maximum total accuracies improve. The total average accuracies are still between 50 % and 70 %, but for the Norway spruce trees, that have sufficient samples from both types of forests, the average classification accuracy is over 80 % and the maximum over 90 % for some of the methods. For the other two species, which don't have training data from the mixed-species forests, the average and maximum accuracies either stay the same or decrease.

Fig. 8 illustrates values for two of the classification features for the trees from both the single-species and mixed-species forest plots. As the number of samples for two of the species is so low it is hard to make definite conclusions, but at least for the two visualized dimensions the species separation seems lower. Especially, mixed-species plot Silver birches overlap with single-species plot Scots pines and mixed-species plot pines overlap with both mixed and single-species plot Norway spruce trees.

4 Discussion

The feature combination test with the three Punkaharju single-species plots showed that, with comprehensive training data, it is possible to find a feature combination for each of the classification methods such that the average classification accuracy is over 93 %. However, when the size of the training data set was more limited, as it would likely be in real applications, the differences in the classification methods started to show. The fact that with only 30 samples per species, the *minimum* accuracy for the SVM$_{lin}$ method was above 83 %, shows

promise for real applications; Sufficient training data can be obtained from the same forest through manual classification. Alternatively, if applicable training data are already available, a complete forest can be classified in a fully automatic procedure, where the classification of a single tree takes only a fraction of a second after the QSM has been computed.

A preliminary mixed-species plot classification test was performed on a limited dataset. When the training data only included samples from single-species forests and neither the classification method parameters or the feature combinations were optimized, the classification accuracies remained low. However, by including samples of Norway spruce trees from both the mixed and single-species plots in the training data the classification accuracy improved significantly, especially for the Norway spruce species. The result suggests that accurate species classification is possible also in mixed-species forests when adequate training data are available. However, it is clear that further testing is needed to determine the classification performance in a mixed-species forest, when suitable data become available.

Even though the tree separation was not perfect as even coarse errors did occur, all of the classification methods were able to classify trees with an accuracy over 94 %, with some feature combinations in the cross-validation test. This shows that the selected features are robust in terms of the tree separation, and that the classification methods are suitable and robust for this classification problem. Furthermore, three of the methods, 4-NN, MNR and SVM$_{lin}$, performed very well and gave consistent results when studying the effect of the size of the training data set, which shows that QSMs contain sufficient species-specific characteristics for classification.

Three species were considered in this study, but the computation of the proposed tree features and the use of the classification methods should generalize well to a larger number of species. In the future, the tests should be repeated with a larger number of species from varying types of forests to see, whether the accuracy also generalizes. It is well known that the top parts of tall trees are poorly covered in TLS measurements, especially in dense environments. Naturally, QSMs inherit this shortcoming, and thus if the differences between two tree species are mainly focused on the top parts of the trees, the proposed classification method might fail to separate them. A further study could also include testing for the effect of leaves on the classification accuracy. From previous studies we know that the presence of leaves will decrease the quality of the QSM, but the effect on species classification still remains unknown.

The QSMs used in this paper were not optimized, but a reasonable set of input parameters was used for all trees. A further study on the effects of the input parameters on the classification should be carried out. One would expect that more accurate QSMs will improve the classification accuracy. The QSMs used in this study consisted of circular cylinders, but similar models can be computed with other, more complicated elements as well (Åkerblom et al., 2015). The use of more complex shapes might give access to even more tree features, such as cross-section shapes, but can decrease the reconstruction accuracy and stability. In any case, the presented results show even the relatively simple circular cylin-

Table 7: Average and maximum classification accuracies for each classification method for the mixed species forest plot in percentages. First half shows results with single-species plot training data and the second half with a combination of single and mixed-species plot training data. The highest maximum total classification accuracies for both types of training data have been highlighted in green, and the maximum accuracies for the Norway spruce trees have been highlighted in black.

Training data	Method	Average				Maximum			
		Total	Birch	Pine	Spruce	Total	Birch	Pine	Spruce
Single	4-NN	48.9	18.7	39.8	52.6	61.0	36.4	61.5	67.3
	MNR	54.6	41.5	58.9	55.7	**76.3**	72.7	92.3	80.4
	SVM$_{lin}$	52.9	29.5	42.9	55.9	64.7	50.0	61.5	71.5
	SVM$_{pol}$	55.8	19.0	50.0	59.9	73.1	36.4	84.6	79.9
	SVM$_{rbf}$	55.1	24.5	43.1	59.0	67.5	40.9	84.6	73.4
Single + Mixed	4-NN	52.7	18.3	33.2	61.6	67.1	36.4	53.8	**79.8**
	MNR	70.3	39.2	34.1	80.4	**81.2**	68.2	53.8	**93.0**
	SVM$_{lin}$	66.3	29.2	28.5	77.8	74.5	50.0	38.5	**88.6**
	SVM$_{pol}$	68.8	18.9	33.2	82.5	75.2	27.3	46.2	**92.1**
	SVM$_{rbf}$	68.2	24.3	29.5	81.1	73.8	40.9	38.5	**89.5**
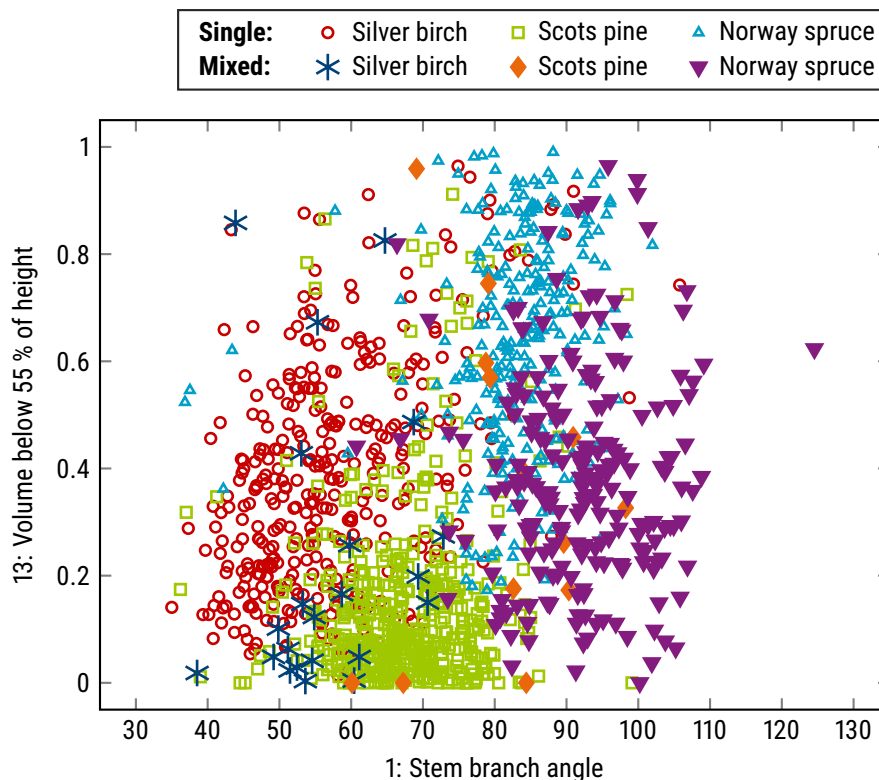
Figure 8: Mixed-species plot species separation with two classification features.

der QSMs can produce high classification accuracies.

The presented 15 classification features yielded good results, but the use of QSMs allows the computation of numerous other features as well. It is also possible to combine the features computed from QSM with features computed directly from the spatial point cloud, or hyper-spectral data, to achieve even better separation between species. However, in comparison to previous studies (Puttonen et al., 2010, 2011), the presented QSM based approach produced similar or even higher classification accuracies without using hyperspectral data or even TLS intensity values. Furthermore, the proposed classification method is fully automatic and works on a lower resolution scanning data than the bark texture based method proposed by Othmani et al. (2013).

Optimization can also be done by increasing the number of scan positions, or, e.g., by elevating the scanner to get better coverage in higher tree parts. The improvement in the scan detail will translate to the quality of the reconstructed models. Alternatively, it could be studied how high classification accuracies can be achieved by using a more coarse scanning setup. It might be possible to integrate automatic species identification to forest inventories done with TLS if the classification features are chosen correctly.

5 Conclusion

We have presented a novel, fully automatic tree species classification approach for terrestrial laser scanning data. The approach is based on reconstructing quantitative structure models (QSM) of the trees, which enables the computation of tree properties that have not been available before for species classification. 15 classification features that utilize the geometry and topology stored in the QSMs were proposed, and their suitability for separating tree species was studied in various tests using three different classification methods: 4 nearest neighbours (4-NN), multinomial regression (MNR) and support vector machines. For the latter, three different kernel functions were also considered: linear (SVM$_{lin}$), polynomial (SVM$_{pol}$), and radial basis function (SVM$_{rbf}$).

The classification accuracy was tested on tree models reconstructed from three single-species forest plots. Over 1,000 trees were used in a 10-fold cross-validation classification test with all classification methods. Furthermore, all possible feature combinations were tested, and the best classification accuracy, 96.9 %, was achieved with the 4-NN method and 10 features. *With the feature count between 6 and 15, it was possible to find a feature combination that resulted in an average classification accuracy above 93 % for all the methods.*

To further test the performance of the classification methods, 126 of the top feature sets were selected to test how the amount of training data affected the classification accuracy. The training and testing trees were selected randomly from the total tree population, and the process was repeated ten times for each feature combination and classification method. The results showed that 4-NN, MNR and SVM$_{lin}$ gave consistent results with all the sets, and were able to classify trees with an average accuracy above 90 % and minimum accuracy over 82 %, with the training sample number per species greater or equal to 30. The SVM$_{pol}$ and SVM$_{rbf}$ methods had lower minimum accuracies as they did not perform well with all of the top feature sets. Thus, more caution should be exercised when selecting feature sets for these particular methods.

Preliminary testing on mixed-species forest plot trees showed that training data collected solely from single-species forest plots is not sufficient for good results. Although, more testing is required when more comprehensive training data becomes available, adding training data from mixed-species forest plots even for just one species improved the classification accuracy to be over 80 % for the MNR method.

Our study showed that tree features made accessible through QSM reconstruction can outperform the existing tree species classification approaches based only on 3D spatial, or hyper-spectral, point cloud data. QSMs provide access to features based on detailed geometry and branching structure making the source data more than three-dimensional. The study also showed that QSMs provide a very robust basis for classification with little need for tuning. Three different methods could accurately and with small variation classify the trees based on QSMs that were not optimized for each tree and with considerable errors in the tree separation. Finally, the proposed species recognition approach is fully automatic because the required pre-processing steps of tree separation of the underlying forest plot (Raumonen et al., 2015) and the QSM reconstruction are automatic.

References

Agresti, A. (1990). *Categorical Data Analysis*. Wiley Series in Probability and Statistics. Wiley.

Åkerblom, M., Raumonen, P., Kaasalainen, M., and Casella, E. (2015). Analysis of geometric primitives in quantitative structure models of tree stems. *Remote Sensing*, 7(4):4581–4603.

Calders, K., Disney, M., Nightingale, J., Origo, N., Barker, A., Raumonen, P. A., Lewis, P., Burt, A., Brennan, J., and Fox, N. (2015a). Traceability of essential climate variables through forest stand reconstruction with terrestrial laser scanning. In *Proceedings of SilviLaser 2015*, pages 122–124.

Calders, K., Newnham, G., Burt, A., Murphy, S., Raumonen, P., Herold, M., Culvenor, D., Avitabile, V., Disney, M., Armston, J., and Kaasalainen, M. (2015b). Nondestructive estimates of

above-ground biomass using terrestrial laser scanning. *Methods in Ecology and Evolution*.

Chang, C.-C. and Lin, C.-J. (2011). LIBSVM: A library for support vector machines. *ACM Transactions on Intelligent Systems and Technology*, 2:27:1–27:27. Software available at http://www.csie.ntu.edu.tw/~cjlin/libsvm.

Derome, J., Lindgren, M., Merilä, P., Beuker, E., and Nöjd, P. (2002). Forest condition monitoring under the UN/ECE and EU programmes in Finland. *Forest Condition Monitoring in Finland – National Report*, 2005:11–20.

Haala, N., Reulke, R., Thies, M., and Aschoff, T. (2004). Combination of terrestrial laser scanning with high resolution panoramic images for investigations in forest applications and tree species recognition. *ISPRS working Group*, 1.

Hackenberg, J., Spiecker, H., Calders, K., Disney, M., and Raumonen, P. (2015). SimpleTree—An Efficient Open Source Tool to Build Tree Models from TLS Clouds. *Forests*, 6(11):4245–4294.

Holopainen, M., Kankare, V., Vastaranta, M., Liang, X., Lin, Y., Vaaja, M., Yu, X., Hyyppä, J., Hyyppä, H., Kaartinen, H., Kukko, A., Tanhuanpää, T., and Alho, P. (2013). Tree mapping using airborne, terrestrial and mobile laser scanning – A case study in a heterogeneous urban forest. *Urban Forestry & Urban Greening*, 12(4):546 – 553.

Lin, Y. and Herold, M. (2016). Tree species classification based on explicit tree structure feature parameters derived from static terrestrial laser scanning data. *Agricultural and Forest Meteorology*, 216:105 – 114.

Meier, I. C., Leuschner, C., Marini, E., and Fender, A.-C. (2016). Species-specific effects of temperate trees on greenhouse gas exchange of forest soil are diminished by drought. *Soil Biology and Biochemistry*, 95:122 – 134.

Merilä, P., Mustajärvi, K., Helmisaari, H.-S., Hilli, S., Lindroos, A.-J., Nieminen, T. M., Nöjd, P., Rautio, P., Salemaa, M., and Ukonmaanaho, L. (2014). Above-and below-ground N stocks in coniferous boreal forests in Finland: Implications for sustainability of more intensive biomass utilization. *Forest Ecology and Management*, 311:17–28.

Othmani, A., Lew Yan Voon, L., Stolz, C., and Piboule, A. (2013). Single tree species classification from terrestrial laser scanning data for forest inventory. *Pattern Recognition Letters*, 34(16):2144–2150.

Possen, B. J., Anttonen, M. J., Oksanen, E., Rousi, M., Heinonen, J., Kostiainen, K., Kontunen-Soppela, S., Heiskanen, J., and Vapaavuori, E. M. (2014). Variation in 13 leaf morphological and physiological traits within a silver birch (Betula pendula) stand and their relation to growth. *Canadian Journal of Forest Research*, 44(6):657–665.

Puttonen, E., Jaakkola, A., Litkey, P., and Hyyppä, J. (2011). Tree classification with fused mobile laser scanning and hyperspectral data. *Sensors*, 11(5):5158–5182.

Puttonen, E., Suomalainen, J., Hakala, T., Räikkönen, E., Kaartinen, H., Kaasalainen, S., and Litkey, P. (2010). Tree species classification from fused active hyperspectral reflectance and {LIDAR} measurements. *Forest Ecology and Management*, 260(10):1843 – 1852.

Rajala, T., Peltoniemi, M., Pennanen, T., and Mäkipää, R. (2012). Fungal community dynamics in relation to substrate quality of decaying Norway spruce (Picea abies [L.] Karst.) logs in boreal forests. *FEMS Microbiology Ecology*, 81(2):494–505.

Raumonen, P., Casella, E., Calders, K., Murphy, S., Åkerblom, M., and Kaasalainen, M. (2015). Massive-scale tree modelling from TLS data. *ISPRS Annals of Photogrammetry, Remote Sensing and Spatial Information Sciences*, II-3/W4:189–196.

Raumonen, P., Kaasalainen, M., Åkerblom, M., Kaasalainen, S., Kaartinen, H., Vastaranta, M., Holopainen, M., Disney, M., and Lewis, P. (2013). Fast automatic precision tree models from terrestrial laser scanner data. *Remote Sensing*, 5(2):491–520.

Vauhkonen, J., Hakala, T., Suomalainen, J., Kaasalainen, S., Nevalainen, O., Vastaranta, M., Holopainen, M., and Hyyppa, J. (2013). Classification of spruce and pine trees using active hyperspectral LiDAR. *IEEE Geoscience and Remote Sensing Letters*, 10(5):1138–1141.